Acta Cryst. (1970). A26, 447

Thermal Diffuse Scattering in Integrated Intensities of Bragg Reflections

BY C. B. WALKER AND D. R. CHIPMAN

Army Materials and Mechanics Research Center, Watertown, Massachusetts 02172, *U.S.A.*

(*Received* 13 *August* 1969)

Two programs have been developed to calculate the one-phonon thermal diffuse scattering included in measured integrated intensities of Bragg reflections for cubic crystals. Both include the anisotropy of the diffuse scattering correctly within the continuum elasticity approximation, and both allow an approximate inclusion of the effects of the wavelength distribution of the primary beam. One program, restricted to ω-scans, includes primary beam divergences approximately using three experimental reflection profiles to describe the weighting function in reciprocal space. The second program, applicable to both ω-scans and θ:2θ-scans, neglects the primary beam divergences but has the advantage of being approximately two orders of magnitude faster than the first. Calculations have been made with these programs for several cases to illustrate the dependence of the included thermal diffuse scattering correction on various factors and to compare with the values obtained from previous approaches.

Introduction

Measurements of integrated intensities of Bragg reflections from a single crystal generally must be corrected for included thermal diffuse scattering if accurate values are required, since this diffuse scattering peaks strongly at the reciprocal lattice points and is not eliminated by the usual background subtraction. An accurate calculation of this correction is quite difficult, as is seen from the recent review by Cochran (1969); and the methods developed by Cooper & Rouse (1968) and Skelton & Katz (1969), while more realistic than the earlier approaches of Nilsson (1957), Annaka (1962), and Pryor (1966), still have retained two major approximations: (*a*) the thermal diffuse scattering is assumed to be spherically symmetric about a reciprocal lattice point, neglecting both possible elastic anisotropy and the non-sphericity arising from the differences between longitudinal and transverse mode contributions; and (*b*) the effects of primary beam divergences and wavelength distributions and of sample mosaic spread are ignored. The present work offers an improvement on both of these points, in that the anisotropic nature of the scattering is included correctly (within the long wavelength, continuum elasticity approximation) and the wavelength distribution and angular divergences of the primary beam are treated by first order approximations. It still is restricted to one-phonon scattering by acoustic modes of small wave-vector and to crystals of cubic symmetry.

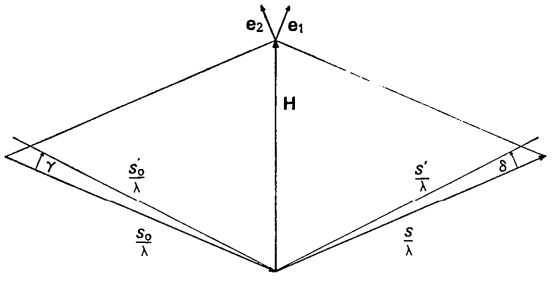

Fig. 1. Geometry of the experiment in the plane of diffraction.

Theory 1

The finite resolution in an actual experimental set-up causes the power received by a fixed detector for a fixed crystal orientation to be proportional to a weighted average of the crystal's intensity distribution over a volume in reciprocal space surrounding the point specified by the mean incident and scattered beam wave vectors. The weighting function (or resolution function) for this averaging represents the combined effects of all the contributing instrumental factors, and its analytical form can be quite complicated, so in general it seems more practical to describe it by means of experimental measurements. The weighting function varies with scattering angle, however, so we have looked for an approximate method of description that would avoid requiring separate sets of measurements for each different angle.

Fig. 1 sketches the usual experimental geometry in the plane of diffraction. Unit vectors $\mathbf{s}_0$ and $\mathbf{s}$ represent the mean directions of the incident and scattered radiation, respectively; λ is the mean wavelength; angles γ and β (not shown), lying in and perpendicular to the diffraction plane, respectively, measure the difference in direction of a particular incident ray, $\mathbf{s}_0'$, from that of $\mathbf{s}_0$; and angles δ and ζ (not shown), in and perpendicular to the plane, respectively, measure the difference in direction of a particular scattered ray, $\mathbf{s}'$, from that of $\mathbf{s}$. The mean diffraction vector is

$$\mathbf{H}=(\mathbf{s}-\mathbf{s}_0)/\lambda \qquad (1)$$

and the diffraction vector for radiation of wavelength, λ_i, and directions $\mathbf{s}_0'$ and $\mathbf{s}'$ is

$$\mathbf{H}'=\mathbf{H}+\mathbf{\Delta} \qquad (2)$$

where, for small divergences and wavelength differences,

$$\mathbf{\Delta} \simeq \frac{\gamma}{\lambda}\mathbf{e}_1+\frac{\delta}{\lambda}\mathbf{e}_2+\frac{\varepsilon}{\lambda}\mathbf{e}_3-\frac{(\lambda_i-\lambda)}{\lambda}\mathbf{H}. \qquad (3)$$

The $[\mathbf{e}_i]$ are a non-orthogonal set of unit vectors, with $\mathbf{e}_1$ and $\mathbf{e}_2$ both in the diffraction plane, $\mathbf{e}_1 \perp \mathbf{s}_0$, $\mathbf{e}_2 \perp \mathbf{s}$, and $\mathbf{e}_3$ (not shown) perpendicular to the plane; and $\varepsilon=\beta+\zeta$.

The form of equation (3) suggests our approximation. We assume that the weight at a point $\mathbf{q}$ with respect to the mean diffraction vector $\mathbf{H}$ can be written as

$$w(\mathbf{H}, \mathbf{q}) = \sum_i A\left(\mathbf{q} + \frac{\lambda_i - \lambda}{\lambda}\mathbf{H}\right) \cdot f_L(\lambda_i) , \qquad (4)$$

where

$$A(\mathbf{p}) = f_1(p_1) \cdot f_2(p_2) \cdot f_3(p_3) \qquad (5)$$

for

$$\mathbf{p} = p_1\mathbf{e}_1 + p_2\mathbf{e}_2 + p_3\mathbf{e}_3 . \qquad (6)$$

The experiment is then completely described in terms of a wavelength distribution function, f_L, and three 'divergence' distribution functions f_1, f_2, and f_3, to be measured by appropriate scans through reflections, and these four functions are considered to be independent of scattering angle. This method of description is accurate, provided crystal mosaic spread and irradiated dimensions are negligible, divergences and relative wavelength spread are small, the detector area is rectangular and has uniform sensitivity, and the primary beam power distribution can be written as the product, $G(\gamma) \cdot B(\beta) \cdot L(\lambda_i)$. It seems to be a reasonable first approximation to many real experiments.

The scattered power received by a fixed detector for a fixed crystal orientation is then given as

$$P = I_e R^2 \frac{\lambda^3}{\sin 2\theta} \iiint w(\mathbf{H}, \mathbf{q}) J(\mathbf{H}+\mathbf{q}) \mathrm{d}^3\mathbf{q} , \qquad (7)$$

where $J(\mathbf{H}+\mathbf{q})$ is the intensity in electron units of the scattering under consideration at the point, $\mathbf{H}+\mathbf{q}$, in reciprocal space; I_e is the electron unit, the intensity of scattering by a free electron; R is the distance from sample to detector; 2θ is the scattering angle; and the functions defining $w(\mathbf{H}, \mathbf{q})$ in equations (4)–(6) have been normalized so that

$$\begin{aligned} \sum_i f_L(\lambda_i) &= 1 \\ \lambda \int f_1(p_1)\, \mathrm{d}p_1 &= 1 \\ f_2(0) = f_3(0) &= 1 \end{aligned} \qquad (8)$$

Note that our diffraction vectors and reciprocal space quantities do not include the factor, 2π, that is incorporated there in some systems of notation (*e.g.* Cochran, 1969).

Consider now the integrated scattering, E, measured in either an ω-scan or a θ:2θ-scan,* where the crystal rotates about $\mathbf{e}_3$ with constant angular velocity, ω, through a small angle, Ω, which takes it through the reflecting position for a Bragg reflection with reciprocal lattice vector, $\boldsymbol{\tau}$. We describe this in terms of a displacement, $\mathbf{r} = r\mathbf{e}_r$, of the weighting function through reciprocal space at a constant velocity, $\dot{r}\mathbf{e}_r$,

$$\begin{aligned} E &= \int P \, \mathrm{d}t \\ &= I_e R^2 \frac{\lambda^3}{\sin 2\theta} \iiiint w(\boldsymbol{\tau}, \mathbf{q} - r\mathbf{e}_r) J(\boldsymbol{\tau}+\mathbf{q}) \mathrm{d}^3\mathbf{q} \frac{\mathrm{d}r}{\dot{r}} , \end{aligned} \qquad (9)$$

* Also sometimes called Ω:2θ-scan.

where $\mathbf{e}_r$ is a unit vector in the direction of motion and r ranges from $r_i < 0$ to $r_f > 0$. For ω-scans, $\mathbf{e}_r \parallel (\boldsymbol{\tau} \times \mathbf{e}_3)$ and $\dot{r} = \omega(2 \sin\theta)/\lambda$, and for θ:2θ-scans, $\mathbf{e}_r \parallel \boldsymbol{\tau}$ and $\dot{r} = \omega(2 \cos\theta)/\lambda$. Rearranging terms and putting $\dot{r} = \omega b_r$, we obtain

$$E = \frac{I_e R^2}{\omega} \frac{\lambda^3}{\sin 2\theta} \iiint W(\boldsymbol{\tau}, \mathbf{q}) J(\boldsymbol{\tau}+\mathbf{q}) \mathrm{d}^3\mathbf{q} \qquad (10)$$

where

$$W(\boldsymbol{\tau}, \mathbf{q}) = b_r^{-1} \int w(\boldsymbol{\tau}, \mathbf{q} - r\mathbf{e}_r) \, \mathrm{d}r . \qquad (11)$$

The function $W(\boldsymbol{\tau}, \mathbf{q})$ gives the integrated weight acting on the point $\boldsymbol{\tau}+\mathbf{q}$ as the weighting function, w, moves through reciprocal space. It measures the fraction of the incident beam that can scatter into the detector with the diffraction vector extending to the point $\boldsymbol{\tau}+\mathbf{q}$ in the crystal's reciprocal space during the scan, and it has the value unity whenever the entire incident beam can so contribute. For an ideal experiment, with no instrumental factors other than a finite receiver slit, W is unity throughout the volume in reciprocal space around $\boldsymbol{\tau}$ 'swept out' by the receiving slit during the scan and is zero elsewhere, while for a real experiment, with the same scan and slits, W is unity through a smaller volume around $\boldsymbol{\tau}$ and varies continuously from one to zero over some region surrounding this inner volume, the details of which depend on the weighting function of the actual experiment.

The integrated intensity of the Bragg reflection measured during this scan is obtained by using the delta function-like crystal interference function for $J(\boldsymbol{\tau}+\mathbf{q})$ in equation (10). Since $W(\boldsymbol{\tau}, \mathbf{q}) = 1$ wherever this $J(\boldsymbol{\tau}+\mathbf{q})$ is non-zero if the entire reflection is to have been measured, the integration is just the usual one (James, 1948), giving

$$E_B = \frac{I_e R^2}{\omega} \frac{\lambda^3}{\sin 2\theta} \frac{N|F|^2}{v} , \qquad (12)$$

where N is the number of unit cells in the crystal, v is the volume of a unit cell, and F is the structure factor of the reflection at $\boldsymbol{\tau}$.

The integrated diffuse scattering measured during this scan can then be written

$$E_D = E_B \frac{v}{N|F|^2} \iiint W(\boldsymbol{\tau}, \mathbf{q}) J_D(\boldsymbol{\tau}+\mathbf{q}) \mathrm{d}^3\mathbf{q} , \qquad (13)$$

where $J_D(\boldsymbol{\tau}+\mathbf{q})$ is the intensity in electron units of the diffuse scattering at the point $\boldsymbol{\tau}+\mathbf{q}$ in reciprocal space.

An integrated background often subtracted from such a measurement is obtained by multiplying the average of the background rates at the ends of the scan by the scan time, Ω/ω. From equations (7) and (12) this can be written

$$\begin{aligned} E'_D = E_B \frac{v}{N|F|^2} \Omega \iiint \tfrac{1}{2}[&w(\boldsymbol{\tau}, \mathbf{q} - r_i\mathbf{e}_r) \\ &+ w(\boldsymbol{\tau}, \mathbf{q} - r_f\mathbf{e}_r)] J_D(\boldsymbol{\tau}+\mathbf{q}) \, \mathrm{d}^3\mathbf{q} . \end{aligned} \qquad (14)$$

We confine our attention now to one-phonon thermal diffuse scattering from acoustic modes, neglecting

contributions from optic modes and from multi-phonon processes as being weaker and slower varying and thus probably more effectively eliminated by the usual background subtraction. The scattering at a point, $\tau+\mathbf{g}$, is then due just to phonons in the three acoustic branches with the wave-vector, $\mathbf{g}$. We assume that $|\mathbf{g}|$ is small enough throughout the region of measurement that dispersion can be neglected and that equipartition of energy holds for these modes at the temperature of the measurement. The intensity in electron units of the scattering at the point, $\tau+\mathbf{g}$, is then written

$$J_D(\tau+\mathbf{g})=\frac{N|F|^2}{v}k_BT\cdot\frac{1}{|\mathbf{g}|^2}\sum_j\frac{[(\tau+\mathbf{g})\cdot\mathbf{e}_{gj}]^2}{\varrho V_{gj}^2} \quad (15)$$

where ϱ is the density of the crystal; $\mathbf{e}_{gj}$ is a unit vector in the direction of polarization of the phonon with wave-vector $\mathbf{g}$ in the jth branch ($j=1, 2, 3$); V_{gj} is the velocity of that phonon; and k_B and T are the Boltzmann constant and the absolute temperature, respectively. This expression is exact for X-ray scattering, but it is only approximate for neutron scattering (Cochran, 1963; Willis, 1969).

Equation (15) is valid for crystals of any symmetry, but its use requires a knowledge of the polarization vectors and velocities of phonons of arbitrary wave vector, and to determine these requires solving the equations of continuum elasticity theory for each wave vector. For crystals of cubic symmetry this equation has been manipulated into an alternative form (Waller, 1925; Nilsson, 1957) that avoids the need for explicit solutions of the elasticity equations and thus is more amenable to calculations; the result can be written

$$J_D(\tau+\mathbf{g})=\frac{N|F|^2}{v}k_BT\frac{C(\tau,\mathbf{g})}{D(\mathbf{g})}, \quad (16)$$

where, if we introduce Miller indices, dimensionless wave-vector components, and ratios of elastic constant combinations through the relations,

$$\begin{aligned}
\tau &= h\mathbf{a}_1^*+k\mathbf{a}_2^*+l\mathbf{a}_3^*\\
\mathbf{g} &= g_1\mathbf{a}_1^*+g_2\mathbf{a}_2^*+g_3\mathbf{a}_3^*\\
g^2 &= g_1^2+g_2^2+g_3^2\\
x_1 &= (C_{11}-C_{12}-2C_{44})/C_{44}\\
x_2 &= x_1(C_{11}+C_{12})/C_{11}\\
x_3 &= x_1^2(C_{11}+2C_{12}+C_{44})/C_{11}\\
x_4 &= (C_{12}+C_{44})/C_{11}
\end{aligned} \quad (17)$$

the $\mathbf{a}^*$ being the axes of the cubic unit cell in reciprocal space, then

$$\begin{aligned}
C(\tau,\mathbf{g}) &= \frac{(h^2+k^2+l^2)}{C_{44}}g^4+\left(\frac{1}{C_{11}}-\frac{1}{C_{44}}\right)g^2\\
&\times(h^2g_1^2+k^2g_2^2+l^2g_3^2)+\frac{x_2}{C_{44}}\\
&\times(h^2g_2^2g_3^2+k^2g_3^2g_1^2+l^2g_1^2g_2^2)-\frac{2x_4}{C_{44}}\\
&\times[hkg_1g_2(x_1g_3^2+g^2)+klg_2g_3(x_1g_1^2+g^2)\\
&+lhg_3g_1(x_1g_2^2+g^2)]
\end{aligned} \quad (18)$$

and

$$D(\mathbf{g})=g^6+x_2g^2(g_1^2g_2^2+g_2^2g_3^2+g_3^2g_1^2)+x_3g_1^2g_2^2g_3^2. \quad (19)$$

Note that for elastic isotropy, $x_1=x_2=x_3=0$.

Equations (16)–(19) give a complete description of the diffuse scattering for cubic crystals, including all anisotropic effects, for $|\mathbf{g}|\ll|\mathbf{a}^*|$. It is sufficiently complicated, however, that previous investigators have chosen to approximate this by an isotropic scattering, obtained by averaging equation (16) over all orientations of the wave-vector $\mathbf{g}$, which in our notation has the simple form,

$$\langle J_D(\tau+\mathbf{g})\rangle=\frac{N|F|^2}{v}kT_B(h^2+k^2+l^2)\frac{\mathscr{K}}{3}\cdot\frac{1}{g^2} \quad (20)$$

where the parameter, $\mathscr{K}$, has been evaluated in various ways (Nilsson, 1957; Walker & Chipman, 1969).

Finally, combining equation (16) with equations (13) and (14) and noting that $d^3\mathbf{q}=dg_1dg_2dg_3/v$, we obtain

$$\frac{E_D}{E_B}=\alpha_1=\frac{k_BT}{v}\iiint W(\tau,\mathbf{g})\frac{C(\tau,\mathbf{g})}{D(\mathbf{g})}dg_1dg_2dg_3 \quad (21)$$

and

$$\begin{aligned}
\frac{E_D'}{E_B}=\alpha_1' &= \frac{k_BT}{v}\Omega\cdot\iiint\tfrac{1}{2}[w(\tau,\mathbf{g}-r_i\mathbf{e}_r)\\
&+w(\tau,\mathbf{g}-r_f\mathbf{e}_r)]\frac{C(\tau,\mathbf{g})}{D(\mathbf{g})}dg_1dg_2dg_3
\end{aligned} \quad (22)$$

and the background-corrected, 'measured' integrated intensity, E_M, is related to the Bragg integrated intensity, E_B, by

$$\begin{aligned}
E_M &= E_B(1+\alpha_1-\alpha_1')\\
&= E_B(1+\alpha)
\end{aligned} \quad (23)$$

Calculation 1

We have developed a computer program to calculate the included thermal diffuse scattering correction, α, that treats the diffuse scattering anisotropy properly and the instrumental resolution factors approximately using the methods and equations of the preceding section. The program is restricted to cubic single crystals, to ω-scan measurements, to rectangular receiver slits, and to measurements in which the scan is symmetrical through a reflection and from which a weighted average of the background at the ends of the scan has been subtracted. As stated earlier, the calculation is restricted to one-phonon scattering, to acoustic modes, and to small divergences and scans so that dispersion can be neglected and equipartition of energy assumed.

The program, called *XTALTDS* 6, is written in Fortran IV for an IBM 7094 and is described in detail elsewhere (Walker & Chipman, 1970*a*). It involves a three-dimensional numerical integration (*viz.* equations (21) and (22) combined) for each reflection. The cubic net of positions at which the integrand is evaluated is

chosen so that the reciprocal lattice point, where $\mathbf{g}=0$, is equidistant from the eight nearest positions on the net. This, together with a simple extrapolation procedure, eliminates any difficulty with the singularity in the integrand at $\mathbf{g}=0$. The amount of calculation needed to obtain a desired precision depends on many factors; the results to be presented here, which were calculated to a precision of approximately 0·1 %, used on the average roughly 25,000 points in the integral and 1·5 minutes of IBM 7094 computing time per reflection.

Using this program we have carried out calculations for a number of different 'experiments' to get an idea of how α depends on various factors. Our procedure has been to make the calculations for a basic experiment, with reasonable parameters, and then to investigate how the results change as usually one factor at a time is varied; there are too many variables to make it practical to consider many other combinations. Since the effects of the different factors generally are not independent, it should be recognized that some of these results may not be appropriate for experiments that are very different from this one.

Our basic experiment is the following: (*a*) The primary beam power angular distribution is given by the product, $G(\gamma)\cdot B(\beta)$, where each of these functions is a Gaussian modified to go to zero at $\pm 3\sigma$. The distribution normal to the diffraction plane (hereafter called vertical) has $\sigma_\beta = 0{\cdot}20°$, and the distribution in the diffraction plane (hereafter, horizontal) has $\sigma_\gamma = 0{\cdot}15°$, so the total zero-to-zero vertical and horizontal divergences are, respectively, 1·2° and 0·9°. (*b*) The primary beam is strictly monochromatic, with $\lambda = 0{\cdot}71140$ Å, midway between the wavelengths of Mo $K\alpha_1$ and Mo $K\alpha_2$. (*c*) The receiver slit is square, intercepting a 3·0° angle (*i.e.* $\pm 1{\cdot}5°$) both vertically and horizontally. (*d*) The crystal rotation during the scan is $\Omega = 2{\cdot}5°$. (*e*) The crystal is tungsten, chosen for its nearly perfect elastic isotropy ($2C_{44}/(C_{11}-C_{12}) = 1{\cdot}008$). Its mosaic spread and irradiated dimensions are negligible. Its temperature is 300° K.

The values of the correction, α, calculated for a set of reflections for this basic experiment are plotted as the points in Fig. 2*a* as a function of the sum of the squares of the Miller indices of the reflection. The reflections range from the (200) to the (820). The right-hand boundary of the figure marks the value of $h^2+k^2+l^2$ at which $\theta = 90°$, and the vertical dashed line marks the limit for experiments with a real Mo $K\alpha$ doublet, beyond which a part of the reflection will fall outside the receiver slit. The values of α vary smoothly with increasing $h^2+k^2+l^2$, varying almost linearly over the middle part of the range, and reach a maximum approximately at the doublet experimental limit. Most of the calculations are for a crystal oriented with an [001] axis vertical; a few cases repeated for other orientations or for other reflections with the same $h^2+k^2+l^2$ give relative differences in α of less than 0·1 %, as could be expected from the very small elastic anisotropy. The size of the correction here is unusually small, only approximately 4 % at its greatest, which is a result of the strong elastic constants in tungsten; at the other extreme, had the crystal been lithium or sodium, with their weak elastic constants, the correction would have been greater by a factor of approximately 20.

The smooth curve in Fig. 2(*a*) gives the results calculated for this experiment on adopting the Cooper–Rouse–Skelton–Katz (CRSK) approximations, that is, using a spherically averaged, isotropic scattering and neglecting the primary beam divergences. The CRSK results here agree fairly well overall with the present calculations, but there is a systematic difference, the CRSK results being greater than the present calculations at low angles and less than the present calculations at high angles, the relative difference varying from +16 to −5 %. The angular dependence of this difference arises almost completely from the approximation of using a spherically averaged scattering; the true surfaces of constant scattering for this elastically isotropic crystal are ellipsoidal, not spherical, with two equal, longer ($\sim 1{\cdot}7x$) axes perpendicular to the reciprocal lattice vector [see equations (16)–(19)], and this, together with the angular dependence of the shape of the volume in reciprocal space swept out by the receiver slit during the scan, readily explains the an-

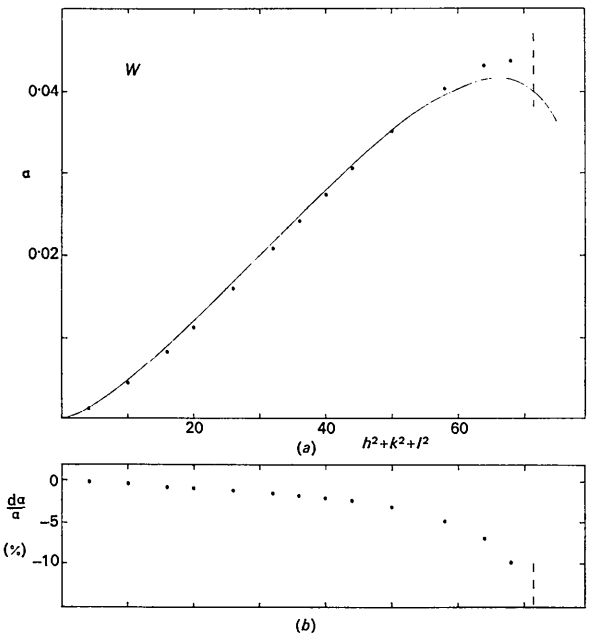

Fig. 2. (*a*) The correction, α, for tungsten reflections, calculated for the basic experiment described in the text, as a function of the sum of the squares of the Miller indices of the reflections. The points are our calculated values, and the smooth curve gives the results calculated with the CRSK approach. The figure boundary at right corresponds to $\theta = 90°$, and the vertical dashed line marks the limiting angle for experiments with Mo $K\alpha$ doublet radiation. (*b*) The percentage change in these values of α when the radiation is changed from one mean wavelength to the two wavelengths of Mo $K\alpha_1$ and Mo $K\alpha_2$.

gular dependence of the error in the CRSK results. The error due to the neglect of the primary beam divergences is smaller and almost independent of angle, as will be discussed below.

Our basic experiment has employed strictly monochromatic radiation in order to facilitate the comparison with the CRSK calculations, where such monochromaticity is assumed. We now let the primary beam have two wavelengths, those of Mo Ka_1 and Mo $K\alpha_2$, each with the same angular distribution of power as before, with weights of $\frac{2}{3}$ and $\frac{1}{3}$, respectively; this should give a reasonable approximation to an experiment with a real Mo $K\alpha$ doublet, where the separation of the lines is approximately 13 times the full width at half maximum of the broader line, and the intensities are as given (Compton & Allison, 1935). The percentage change in the value of α caused by this change from one wavelength to two wavelengths in the experiment is plotted for the different reflections in Fig. 2(*b*). There is a reduction in the value of α for each reflection, and the amount of the reduction increases smoothly and at an increasing rate with increasing angle to approximately 10% at the (820) reflection. The size of this 'two wavelength effect' is such that the values of α for this 'real' experiment are now smaller than the CRSK results [the curve of Fig. 2(*a*)] for all reflections.

Our basic experiment uses a receiver slit 3·0° high and 3·0° wide and a crystal rotation $\Omega=2{\cdot}5°$, these numbers seeming suitable for an experiment with the given primary beam divergences and Mo $K\alpha$ doublet wavelengths that is to be able to measure reflections up to fairly high angles. We consider next how the values of α depend on these three angular quantities, in turn varying each one singly while keeping all other factors of the experiment constant. The percentage change in α found on varying the slit height is given in Table 1 for five representative reflections. One notes that the sensitivity to height changes is small overall, smaller for the low angle reflections, and that it decreases rapidly with increasing height. The percentage change in α found on varying the slit width is given in Table 2 for the same five reflections. The values of α are appreciably less sensitive to width increases than they are to height increases, a change in width from 3·0° to 4·5° increasing the α's 3 to 6 times less than is caused by such a change in the receiver height. The percentage change in α found on varying the amount of crystal rotation is given in Table 3 for four of the reflections. The values of α depend much more strongly on this variable than on the two slit dimensions, and this dependence is almost linear for the low angle reflections. These results for the dependence on slit height, width, and crystal rotation are repeated with generally only minor differences when the calculations are made using the two Mo $K\alpha$ doublet wavelengths instead of the single wavelength.

To investigate the effects of elastic anisotropy, we change the sample to a single crystal of β'-CuZn with 51·86 at.% Cu, for which $2C_{44}/(C_{11}-C_{12})=9{\cdot}21$

Table 1. *The percentage change in α for five reflections caused by varying the slit height in the basic experiment*

$h^2+k^2+l^2$	4	16	36	50	64
Height (°)					
6·0	1·6	4·8	7·9	8·8	8·4
4·5	1·2	3·7	5·8	6·3	6·1
3·0	0	0	0	0	0
1·5	−6·5	−14·3	−18·5	−19·2	−18·5

Table 2. *The percentage change in α for five reflections caused by varying the slit width in the basic experiment*

$h^2+k^2+l^2$	4	16	36	50	64
Width (°)					
4·5	0·1	1·0	1·9	1·9	1·0
3·0	0	0	0	0	0
1·5	−1·2	−5·8	−11·6	×	×

Note: × indicates that part of the Bragg reflections of a Mo $K\alpha$ doublet will fall outside the slit.

Table 3. *The percentage change in α for four reflections caused by varying the amount of crystal rotation in the basic experiment*

$h^2+k^2+l^2$	16	36	50	64
Ω(°)				
6·0	88·4	63·9	52·8	41·7
5·0	69·4	52·7	44·6	35·8
4·0	46·0	37·0	32·4	27·0
3·5	32·0	26·7	24·0	20·6
3·0	16·8	14·5	13·4	12·0
2·5	0	0	0	0
2·0	−18·3	−16·8	−16·4	−16·4
1·5	−38·3	−35·9	−35·5	× ×
1·0	× ×	× ×	× ×	× ×

Note: × × indicates that the crystal rotation is not sufficient to Bragg reflect all of the primary beam for a Mo $K\alpha$ doublet.

(McManus, 1963), retaining the other factors of the basic experiment. The values of α calculated for a series of reflections for this experiment are plotted as the points in Fig. 3(*a*) as a function of the sum of the squares of their Miller indices. As in Fig. 2, the right boundary of the figure marks the abscissa value at which $\theta=90°$, and the dashed line marks the limit for experiments with a real Mo $K\alpha$ doublet. In contrast to the results for tungsten, the values of α for this anisotropic crystal vary quite irregularly with increasing $h^2+k^2+l^2$ and depend on the orientation of the crystal for each reflection. The calculations for a majority of the reflections have been given for two different orientations and calculations have been included for different reflections with the same value of $h^2+k^2+l^2$ to illustrate the spread in the possible values of α at a given $h^2+k^2+l^2$ produced by the elastic anisotropy. One sees that this spread can be quite large; for example, the value of α for a (622) reflection here is 0·124 if an $[0\bar{1}1]$ direction is vertical and is 0·169 for a $[\bar{2}33]$ vertical. The substantial size of the value of α should also be noted. The smooth curve gives the results obtained for this experiment with CRSK-type calcula-

tions. It does not form a very good approximation to the present calculations; its spherical averaging precludes any crystal orientation dependence, and it seems to give somewhat higher values for most reflections than the averages of our calculations, so relative differences of over 20% can be found at most angles and differences of over 40% can be found in a number of instances.

The percentage change in the values of α for this β'-CuZn experiment found on using the two Mo $K\alpha$ doublet wavelengths instead of the single wavelength are plotted for the different reflections and various crystal orientations in Fig. 3(*b*). As in the case for tungsten, there is generally a reduction in the value of α for each reflection, but anisotropy causes this to vary quite irregularly for the different reflections and for different crystal orientations. In fact, in the case of the (622) reflection used in the example above, this two-wavelength effect reduces the value of α by 2·9% if the $[\bar{2}33]$ direction is vertical, but it actually increases the value of α by 0·6% if the $[0\bar{1}1]$ is vertical.

Finally, to investigate the effect of the angular divergences of the primary beam, we have compared the values of α for tungsten obtained with the basic experiment primary beam angular distributions, using the two Mo $K\alpha$ doublet wavelengths, the basic receiver slit, and varying amounts of crystal rotation, with the corresponding values of α obtained when the primary beam divergences are set equal to zero, all other factors remaining the same. The percentage change in α found on changing to the primary beam with zero angular divergence is given as a function of the amount of crystal rotation in Table 4 for four representative reflections. One notes the very interesting result that these changes in α are really quite small for all except small amounts of crystal rotation, and they are approximately the same for all reflections. The effect of the primary beam divergences here becomes appreciable only when the crystal rotation is not much larger than the minimum amount needed to Bragg reflect all of the primary beam. The effect is of course a function of the other experimental factors too, but the few cases that we have checked indicate that, for conditions that are not extreme, the effect generally remains small; for example, repeating the comparison for a crystal rotation, $\Omega = 2{\cdot}5°$, but with a slit height of 1·5° instead of 3·0°, we find that the average percentage change in α on eliminating the primary beam divergences is 3·3%, where the change for the 3·0° slit height was 1·9%. Note that in this second example the slit height is only 0·3° greater than the total vertical spread of the primary beam. The effect also depends somewhat on the sample; we have repeated this comparison using the basic slit and a crystal rotation, $\Omega = 2{\cdot}5°$, for the anisotropic crystal, β'-CuZn, and find that, while the average percentage change in α is 1·9% as before, the specific change depends much more on the particular reflection and on the crystal orientation and varies between 1·0 and 2·6%.

Table 4. *The percentage change in α for four reflections caused by eliminating the angular divergence of the primary beam of the basic experiment as a function of the amount of crystal rotation*

$h^2+k^2+l^2$ / Ω (°)	16	36	50	64
6·0	0·9	0·9	1·0	1·0
5·0	0·9	1·0	1·0	1·1
4·0	1·1	1·1	1·1	1·2
3·5	1·2	1·2	1·2	1·3
3·0	1·6	1·4	1·5	1·5
2·5	2·1	2·0	1·8	1·9
2·0	2·9	2·9	2·9	3·2
1·5	5·0	5·3	6·7	× ×
1·0	× ×	× ×	× ×	× ×

Note: × × indicates that the crystal rotation is not sufficient to Bragg reflect all of the primary beam for a Mo $K\alpha$ doublet and the basic angular distribution.

Theory 2

The results of the previous paragraph indicate that the neglect of the angular divergences of the primary beam will cause only a small error in the included thermal diffuse scattering correction, α, for a rather wide range of experimental conditions. We consider now how the equations for this correction simplify when such divergences are neglected.

Let the primary beam consist first of just one wavelength, λ_i. The integrated weighting function, $W(\boldsymbol{\tau}, \mathbf{g})$, for the experiment is then unity throughout the (approximately) parallelepiped volume, V_i, swept out by the receiver slit during the scan and is zero elsewhere, so equation (21) becomes:

$$\alpha_1 = \frac{k_B T}{v} \iiint_{Vi} \frac{C(\boldsymbol{\tau}, \mathbf{g})}{D(\mathbf{g})} \, dg_1 dg_2 dg_3 \,. \qquad (24)$$

The fixed crystal weighting function, $w(\boldsymbol{\tau}, \mathbf{g})$, has a constant value throughout the rectangular section of infinitesimal thickness defined by the receiver slit and is zero elsewhere. Then, using equation (11), equation (22) can be written

$$\alpha_1' = \frac{k_B T}{v} \cdot \tfrac{1}{2} \frac{a_0}{\lambda} \Omega \sin 2\theta \cdot \sum_{j=1}^{2} \iint_{S_{ij}} \frac{C(\boldsymbol{\tau}, \mathbf{g})}{D(\mathbf{g})} \, dA \qquad (25)$$

where S_{i1} and S_{i2} are the two end faces of V_i corresponding to the start and finish of the scan.

Equation (24) can be reduced further by virtue of the $1/g^2$ dependence of its integrand.* Let $d\Omega$ be a differential solid angle drawn from X, the reciprocal lattice point in V_i, that intercepts a differential area, dA, on the surface of V_i at a distance g from X, with the vector from X to dA that defines the direction of $d\Omega$ making an angle φ with the normal to dA, and let da be the differential area parallel to dA that is intercepted by $d\Omega$ at some smaller distance, q, from X. If

* We thank B.T.M.Willis for the suggestion that this simplification might be possible.

we divide the part of the volume of V_i enclosed by $d\Omega$ into the differential volume elements, $dV = da dq \cos\varphi$, then, since $da \propto q^2$ and since $C(\tau, \mathbf{q})/D(\mathbf{q}) \propto 1/q^2$,

$$\frac{C(\tau, \mathbf{q})}{D(\mathbf{q})} da dq \cos\varphi = \frac{C(\tau, \mathbf{g})}{D(\mathbf{g})} dA dq \cos\varphi ,$$

a constant, independent of q, for all volume elements within $d\Omega$. Integration with respect to q is immediate, and equation (24) becomes

$$\alpha_1 = \frac{k_B T}{v} \iint_{S_i} \frac{C(\tau, \mathbf{g})}{D(\mathbf{g})} g \cos\varphi \, dA \qquad (26)$$

where the integral is over the surface of V_i. Since the surface of V_i is made up of planes, S_{ij}, on each of which $g \cos\varphi = n_j$, the constant perpendicular distance from X to that plane, equation (26) can be written

$$\alpha_1 = \frac{k_B T}{v} \sum_{j=1}^{6} n_j \iint_{S_{ij}} \frac{C(\tau, \mathbf{g})}{D(\mathbf{g})} dA \qquad (27)$$

which is obviously much easier to evaluate than equation (24). The similarity of this equation to equation (25), the expression for the background factor, simplifies the calculation of the combined correction factor, α; indeed, in symmetrical scans with only one wavelength, there is a straight-forward cancellation of terms, since, in the same indexing notation, one has the relation

$$n_1 + n_2 = \frac{a_0}{\lambda} \Omega \sin 2\theta .$$

Finally, if the primary beam contains several wavelengths, one calculates the correction factor for each wavelength, where the appropriate volume V_i for the ith wavelength is obtained by displacing the volume for some central wavelength, λ, by the amount $\tau(\lambda - \lambda_i)/\lambda$, and then sums the appropriately weighted results. This procedure can be shortened if the scan has been symmetrical for the central wavelength (*i.e.* if the reciprocal lattice point X is a center of symmetry for the volume V for the wavelength λ) for then if any two wavelengths, λ_i and λ_j, with arbitrary weights, are equally spaced about λ, that is, if $(\lambda - \lambda_i) = -(\lambda - \lambda_j)$] one only has to calculate the correction for one wavelength and multiply this by the sum of the two weights to obtain the contribution of both. Thus, for example, for symmetrical scans in which the beam has the two Mo $K\alpha$ doublet wavelengths, the correction factor is given by a single calculation in which the volume V_i is shifted parallel to τ by the amount (in our dimensionless units), $(h^2+k^2+l^2)^{1/2} \cdot (\lambda_1 - \lambda_2)/(\lambda_1 + \lambda_2)$.

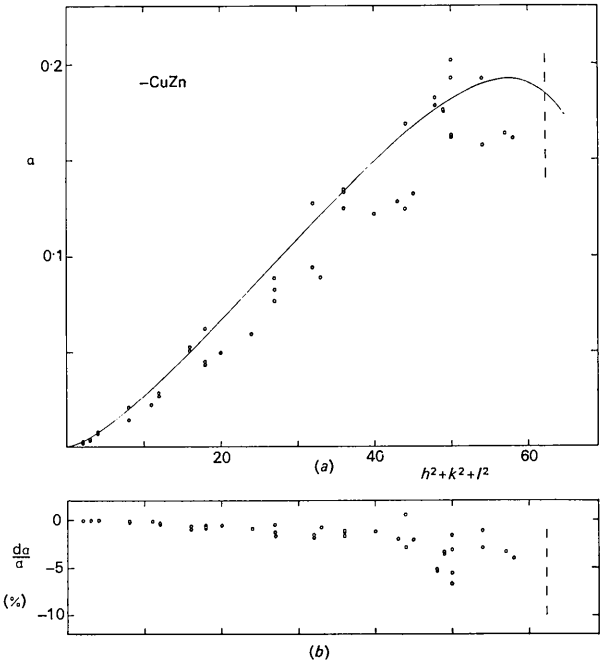

Fig. 3. (*a*) The correction, α, for β'–CuZn reflections, calculated for the basic experiment, as a function of the sum of the squares of the indices of the reflections. The points are our calculated values, given in most cases for two different crystal orientations and for different reflections with the same value of $h^2+k^2+l^2$. The smooth curve gives the results of the CRSK approach. The figure boundary corresponds to $\theta = 90°$, and the vertical dashed line marks the doublet experimental limit. (*b*) The percentage change in these values of α when the radiation is changed from one mean wavelength to the two wavelengths of Mo $K\alpha_1$ and Mo $K\alpha_2$.

Calculation 2

We have developed a second computer program to calculate the correction factor, α, that neglects primary beam divergences but retains the correct treatment of the diffuse scattering anisotropy and allows the approximate inclusion of wavelength distribution effects using the methods and equations of the preceding section. This program is again restricted to cubic single crystals, to rectangular receiver slits, and to measurements in which the scan is symmetrical through the reflection and from which a weighted average of the background at the ends of the scan has been subtracted, but it can treat both ω-scan and θ:2θ-scan measurements. The restrictions on the calculations, one phonon scattering, acoustic modes, *etc.*, are the same as before.

This program, called *XTDS* 2, is written in Fortran IV for an IBM 7094 and is described in detail in a separate report (Walker & Chipman, 1970*b*). It involves a two-dimensional numerical integration [equations (27) and (25) combined] for each reflection. The calculations to be presented here, which were again carried to a precision of approximately 0·1%, used on the average roughly 2,500 points in the integral and approximately 1 second of IBM 7094 computing time per reflection for the basic experiment, which, excluding input/output and other tape operations, represents a gain in speed of approximately two orders of magnitude over the first program.

We have used this program to calculate the values of α for several experiments for both θ:2θ-scans and ω-scans to investigate the dependence on the type of

scan. The basic experiment for these calculations is the same as before, except, of course, that the primary beam now has no angular divergence.

The values of α for a set of reflections for this basic experiment for the $\theta:2\theta$-scan show the same general features as are found for the ω-scan results; they vary smoothly with increasing $h^2+k^2+l^2$, varying almost linearly over the middle part of the range, and reach a maximum at approximately the same angle as that for the ω-scan. The CRSK calculations agree rather more poorly with these values than they do in the ω-scan case; the systematic difference here is such that the CRSK results are smaller than the present values for all but the lowest angle reflection, the relative difference varying from +2% at the (200) reflection to −16% at the (820) reflection. The 'two wavelength effect' causes a reduction in the value of α similar to that found in the ω-scan case, with the magnitude of the reduction for the $\theta:2\theta$-scan more dependent on other parameters such as the amount of crystal rotation; for the basic experiment the reduction is somewhat larger for the $\theta:2\theta$-scan than for the ω-scan, amounting to approximately 13% at the (820) reflection.

A quantitative comparison of the values of α for the two types of scan for this basic experiment is given by the solid curve of Fig. 4, where the ratio of the value of α for the $\theta:2\theta$-scan to that for the ω-scan with the same 2·5° crystal rotation is plotted as a function of $h^2+k^2+l^2$. The $\theta:2\theta$-scan gives values of α considerably larger than those for the ω-scan at low angles, but the ratio changes sufficiently with angle that at the high angles the ω-scan values are the larger. This is an illustration of how the values of α can depend on the type of scan, but it should be emphasized that the result depends quite strongly on the particular factors of the experiment. For example, if we change the amount of crystal rotation to 5·0°, keeping all other factors the same, we find that the ratio of the value of α for the $\theta:2\theta$-scan to that for the ω-scan is given by the long-dashed curve of Fig. 4, quite different from the result for the basic experiment, while if the receiver slit is reduced from 3·0° square to 1·5° square for this 5·0° crystal rotation, keeping all other factors constant, the ratio of the $\theta:2\theta$-scan correction to that for the ω-scan is now given by the short-dashed curve of Fig. 4, different from both of the first two results. This last result is similar to that reported by Skelton & Katz (1969).

Finally, it is interesting to compare more directly how the values of α for this basic experiment depend on the amount of crystal rotation for the two types of scan. Table 3 gave the percentage change in α for ω-scan measurements for four reflections on varying the amount of crystal rotation in the basic experiment, where the primary beam had the divergences described earlier; these results are repeated with only minor differences here, where the primary beam has zero angular divergences. The corresponding percentage changes in α for $\theta:2\theta$-scan measurements are given in Table 5. The changes for the $\theta:2\theta$-scan are somewhat smaller than those for the ω-scan at large rotations, and they are much more sensitive to a change to the two doublet wavelengths, and there is the interesting inversion that in the $\theta:2\theta$-scans the high angle reflections show the almost linear dependence of α on the amount of crystal rotation.

Discussion

Our object in undertaking this work was to develop a method for calculating the correction for included thermal diffuse scattering in single crystal integrated intensity measurements that would treat several physical features of the problem in a more realistic manner than had been done in previous calculations. The approach is summarized in the section *Theory* 1; it includes the anisotropy of the diffuse scattering correctly

Table 5. *The percentage change in α for $\theta:2\theta$-scan measurements of four reflections on varying the amount of crystal rotation in the second basic experiment*

$h^2+k^2+l^2$ / Ω (°)	16	36	50	64
6·0	21·2	31·9	41·8	59·4
5·0	18·9	28·2	36·2	49·6
4·0	15·2	22·0	27·3	35·3
3·5	12·2	17·1	20·7	25·7
3·0	7·6	10·2	11·8	14·0
2·5	0	0	0	0
2·0	−13·6	−14·8	−15·4	−16·4
1·5	−36·8	−34·5	−34·1	−35·1

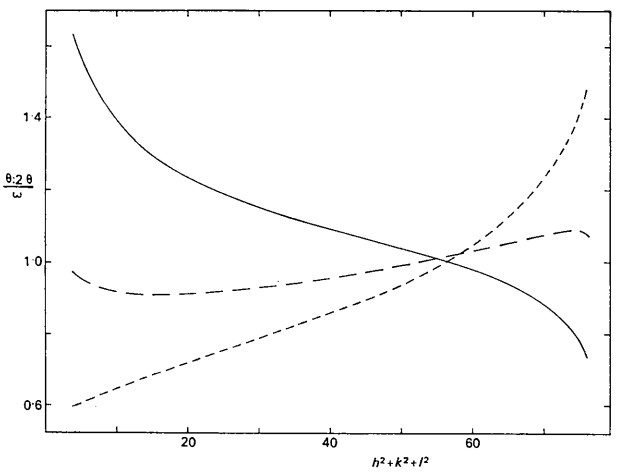

Fig. 4. The ratio of the correction, α, for tungsten reflections measured with a $\theta:2\theta$-scan to that for ω-scan measurements made with the same crystal rotation, as a function of the sum of the squares of the indices of the reflections. The solid line gives the result for the second basic experiment, with a 3·0° square slit and $\Omega=2{\cdot}5°$; the long-dashed curve is obtained if the crystal rotation is changed to $\Omega=5{\cdot}0°$; and the short-dashed curve is obtained when $\Omega=5{\cdot}0°$ and the slit is changed to 1·5° square.

and the divergences and wavelength distribution of the primary beam by a first approximation. The approximate procedure used to include the primary beam characteristics also will include to some extent the effects of the crystal mosaic spread and the irradiated sample dimensions, even though these have not been discussed explicitly, if the experimental divergence distribution functions are measured with reflections from the sample itself. The method is still limited to cubic crystals, because relations equivalent to equation (16) have not yet been derived for crystals of other symmetries, and to one-phonon scattering, and it is more accurate for X-ray scattering than for neutron scattering, where further approximations are required.

A computer program, *XTALTDS* 6, employing this approach, but restricted to ω-scans to simplify the programming, has been developed and used to investigate the dependence of the correction on various factors. These calculations show that the anisotropy of the scattering causes effects that may be significant even for elastically isotropic crystals and that can be quite large and orientation dependent for crystals that are elastically anisotropic. They show also that the doublet nature of the usual X-ray wavelength distribution can cause appreciable effects at the higher angles, a result that should also hold for the broader neutron wavelength distributions usually used. They also yield the very interesting observation that the neglect of the angular divergences of the primary beam in the calculation causes only a small error in the correction for a rather wide range of experimental conditions, those where the slit dimensions and crystal rotation are not too near the minimum values required by the experiment. This suggests that the fine details of the primary beam characteristics are not important in such a calculation, and thus that this program should be able to produce values for the correction accurate to 1% or better for many cases, despite the simplicity of its approximations. It also has led us to develop a different method of calculation for those cases in which the error due to the neglect of the angular divergences of the primary beam can be tolerated; this second approach, summarized in the section *Theory* 2, is the basis for the computer program, *XTDS* 2, which treats both ω-scans and θ:2θ-scans and is approximately two orders of magnitude faster than the first program, *XTALTDS* 6.

Calculations have also been included to show how the correction can vary with other factors such as slit dimensions, amount of crystal rotation, and type of scan. Some of these results, such as the weak dependence on slit height and the even weaker dependence on slit width, are particularly interesting and suggestive as to the design of experiments. However it must again be emphasized that the effects of these various factors are generally not independent, so the results obtained here may turn out to be quite different from the corresponding results for experiments that are very different from this one. This is clearly demonstrated by the strikingly different results for the ratio of the θ:2θ-scan correction to that for the comparable ω-scan for the three experiments plotted in Fig. 4.

One limitation of the present approaches must be made clear. The programs we have developed calculate only the correction for one-phonon scattering, ignoring two-phonon and higher order processes. It seems reasonable to expect that the correction for multi-phonon scattering will be much smaller than that for one-phonon scattering, but no quantitative measure of their relative sizes has yet been determined. Thus, when the correction for one-phonon scattering is large, the neglect of the multi-phonon contribution may be a significant source of error when very accurate results are required.

The two approaches developed here are certainly more accurate than any other approach that has previously been used, but they are also more complex and more costly to use, since they involve numerical integration in either three dimensions (*XTALTDS* 6) or two dimensions (*XTDS* 2). The best of the previous approaches is that of CRSK, which needs only a one-dimensional numerical integration, and it has been compared with the present calculations to illustrate the errors that can result from this approach. Still simpler, more approximate approaches include using the analytical expression derived by Nilsson, or treating the correction as an error in the Debye–Waller factor. The decision as to which approach to use in making this correction will depend of course on many factors, including the size of the correction, the error that can be accepted, and the cost that can be supported. Our second approach, with the program, *XTDS* 2, or a modification thereof, seems to offer the best combination of accuracy and speed for general purposes.

We are indebted to L. D. Jennings for many helpful discussions.

References

ANNAKA, S. (1962). *J. Phys. Soc. Japan*, **17**, 846.
COCHRAN, W. (1963). *Rep. Progr. Phys.* **26**, 1.
COCHRAN, W. (1969). *Acta Cryst.* A**25**, 95.
COMPTON, A. H. & ALLISON, S. K. (1935). *X-rays in Theory and Experiment*. New York: Van Nostrand.
COOPER, M. J. & ROUSE, K. D. (1968). *Acta Cryst.* A**24**, 405.
JAMES, R. W. (1948). *The Optical Principles of the Diffraction of X-rays*. London: Bell.
MCMANUS, G. M. (1963). *Phys. Rev.* **129**, 2004.
NILSSON, N. (1957). *Ark. Fys.* **12**, 247.
PRYOR, A. W. (1966). *Acta Cryst.* **20**, 138.
SKELTON, E. F. & KATZ, J. L. (1969). *Acta Cryst.* A**25**, 319.
WALKER, C. B. & CHIPMAN, D. R. (1969). *Acta Cryst.* A**25**, 395.
WALKER, C. B. & CHIPMAN, D. R. (1970*a*). AMMRC – Technical Report in preparation.
WALKER, C. B. & CHIPMAN, D. R. (1970*b*). AMMRC – Technical Report in preparation.
WALLER, I. (1925). Uppsala Dissertation.
WILLIS, B. T. M. (1969). *Acta Cryst.* A**25**, 277.